Proceedings of the 17th IASTED International Conference
MODELLING AND SIMULATION
May 24-26, 2006, Montreal, QC, Canada

MODELING OF MASS TRANSFER IN MULTI-PASS MASS EXCHANGERS WITH EXTERNAL RECYCLE

Jr-Wei Tu and Chii-Dong Ho
Department of Chemical and Materials Engineering, Tamkang University
Tamsui, Taipei, Taiwan 251, R.O.C.
cdho@mail.tku.edu.tw

ABSTRACT
The mass transfer in a multi-pass mass exchanger with external recycle has been investigated theoretically. The analytical solutions were obtained by using the orthogonal expansion technique associated with the eigenfunction expanding in terms of an extended power series. The influences of the subchannel thickness ratio β, recycle ratio R, and the parameter of permeable barrier γ on the outlet concentration and mass transfer efficiency were discussed and represented graphically in the present study. The mass transfer efficiency improvement by employing the multi-pass mass exchangers with recycle was defined as the percentage increase in mass-transfer rate, based on that of a single-pass device with same working dimensions and without external recycle and any permeable barrier inserting. Considering both mass transfer efficiency improvement and power consumption increment, an optimal device performance of multi-pass mass exchangers can be obtained with the suitable adjustment of the permeable barrier locations.

KEY WORDS
Mass transfer, external recycle, multi-pass operations, conjugated Graetz problem.

1. Introduction

The studies of the heat transfer process of laminar forced convection inside a bounded conduit under constant wall temperature or heat flux are the classical Graetz problem [1, 2] while the extension of Graetz problem to multiphase or multistream systems with coupling through conjugated conduction-convection conditions at the boundaries is so-called the conjugated Graetz problems [3, 4]. As referred to many investigators, the mass or heat transfer coefficient can be enhanced by scaling down the channel size [5, 6] or dividing an open-duct device into several subchannels [7, 8]. Moreover, the application of the internal or external concept is used widely in the industrial processes such as air-lift reactor [9] and thermal diffusion column [10].

A new design of multi-pass mass exchanger with external recycle is investigated in this study. The mathematical formalisms for such conjugated Graetz problem of multi-pass mass exchangers with external recycle and constant wall concentration were developed. The analytical solutions for such devices were obtained by means of an orthogonal expansion technique with the eigenfunction expanding in power series.

2. Multi-pass devices

Three ideal permeable membrane with negligible thickness $\delta (<< W)$ are inserted into a parallel-plate with thickness W, length L, and infinite width B to divide an open duct into four parts, subchannels a, b, c and d with thickness W_a, W_b, W_c and W_d, respectively, and the subchannel thickness ratio is defined as $\beta = W_a / W_b = W_d / W_c$. The fluid with volume flow rate V and the inlet concentration C_I firstly feeds into the two inner subchannels and exits from two outer subchannels as shown in Fig. 1. Before entering the two outer channels, the fluid will mixed with the outlet fluid with volume flow rate RV and the outlet concentration C_F by the aid of the conventional pumps.

The following assumptions were made in present study: fully-developed laminar flow in each channel, neglecting the entrance length and longitudinal diffusion, ignoring the end effects and concentration polarization phenomena on the idealized membrane, and constant physical properties of fluid. With the aid of those assumptions, the velocity distributions and mass balance equations in dimensionless form for the multi-pass mass exchanger with constant wall concentration can be written as:

$$\frac{\partial^2 \psi_i(\eta_i,\xi)}{\partial \eta_i^2} = \left[\frac{W_i^2 v(\eta_i)}{LD}\right] \frac{\partial \psi_i(\eta_i,\xi)}{\partial \xi}, \quad i = a,b,c,d \qquad (1)$$

$$v_i(\eta_i) = \bar{v}_i(6\eta_i - 6\eta_i^2), \quad 0 \le \eta_i \le 1, \quad i = a,b,c,d \qquad (2)$$

in which

$$\bar{v}_a = [-(R+1)V / W_a B], \quad \bar{v}_b = [V / W_b B], \quad \eta_i = x_i / W_i,$$
$$\bar{v}_c = [V / W_c B], \quad \bar{v}_d = [-(R+1)V / W_d B], \quad \xi = z / L$$
$$\psi_i = (C_i - C_s)/C_I - C_s, \quad \theta_i = 1 - \psi_i, \quad Gz_m = 2VW / DBL \qquad (3)$$

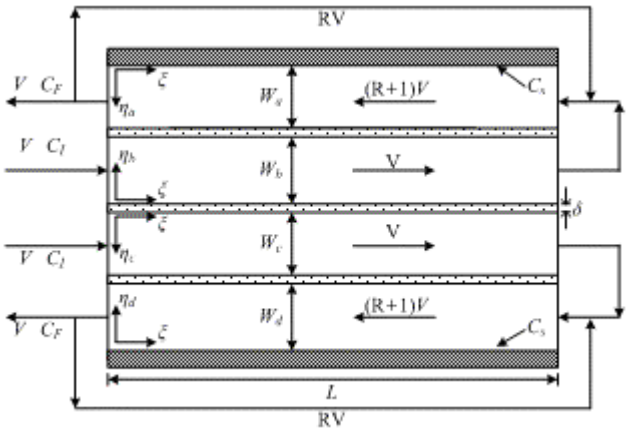

Fig.1 Multi-pass mass exchanger

The corresponding boundary conditions for solving Eqs. (1) and (2) are

$$\psi_a(0,\xi)=0 \tag{4}$$

$$-\frac{\partial\psi_a(1,\xi)}{\partial\eta_a}=\frac{W_a}{W_b}\frac{\partial\psi_b(1,\xi)}{\partial\eta_b} \tag{5}$$

$$\frac{\partial\psi_a(1,\xi)}{\partial\eta_a}=-\frac{\gamma W_a}{W}[\psi_a(1,\xi)-\psi_b(1,\xi)] \tag{6}$$

$$-\frac{\partial\psi_b(0,\xi)}{\partial\eta_b}=\frac{W_b}{W_c}\frac{\partial\psi_c(0,\xi)}{\partial\eta_c} \tag{7}$$

$$\frac{\partial\psi_b(0,\xi)}{\partial\eta_b}=-\frac{\gamma W_b}{W}[\psi_b(0,\xi)-\psi_c(0,\xi)] \tag{8}$$

$$-\frac{\partial\psi_c(1,\xi)}{\partial\eta_c}=\frac{W_c}{W_d}\frac{\partial\psi_d(1,\xi)}{\partial\eta_d} \tag{9}$$

$$\frac{\partial\psi_c(1,\xi)}{\partial\eta_c}=-\frac{\gamma W_c}{W}[\psi_c(1,\xi)-\psi_d(1,\xi)] \tag{10}$$

$$\psi_d(0,\xi)=0 \tag{11}$$

and the dimensionless outlet concentration is

$$\theta_F=1-\psi_F=\frac{C_F-C_I}{C_s-C_I} \tag{12}$$

By following the same calculation procedure performed in the previous work [7, 8], the eigenvalues ($\lambda_1,\lambda_2,....,\lambda_m,...$) can be calculated from Eqs. (13)-(15),

$$\frac{S_{a,m}}{S_{b,m}}=\frac{\gamma W_a F_{b,m}(1)}{\gamma W_a F_{a,m}(1)+W F'_{a,m}(1)}=-\frac{W_a F'_{b,m}(1)}{W_b F'_{a,m}(1)} \tag{13}$$

$$\frac{S_{b,m}}{S_{c,m}}=\frac{\gamma W_b F_{c,m}(0)}{\gamma W_b F_{b,m}(0)+W F'_{b,m}(0)}=-\frac{W_b F'_{c,m}(0)}{W_c F'_{b,m}(0)} \tag{14}$$

$$\frac{S_{c,m}}{S_{d,m}}=\frac{\gamma W_c F_{d,m}(1)}{\gamma W_c F_{c,m}(1)+W F'_{c,m}(1)}=-\frac{W_c F'_{d,m}(1)}{W_d F'_{c,m}(1)} \tag{15}$$

While all of the eigenvalues (λ_m) calculated from Eqs. (13)-(15), the expansion coefficients, ($S_{a,m}$, $S_{b,m}$, $S_{c,m}$ and $S_{d,m}$) and the associated eigenfunctions ($F_{a,m}$, $F_{b,m}$, $F_{c,m}$ and $F_{d,m}$) can be found. The dimensionless outlet concentration $\psi_{F,ab}$ or $\psi_{F,cd}$ which is referred to as the average dimensionless outlet concentration can be determined by

$$\psi_{F,ab}=\frac{-\int_0^1 v_a W_a B\psi_a(\eta_a,0)d\eta_b}{(R+1)V}$$

$$=\frac{-2W}{W_a(R+1)Gz_m}\sum_{m=0}^{\infty}\frac{e^{-\lambda_m}S_{a,m}}{\lambda_m}\{F'_{a,m}(1)-F'_{a,m}(0)\} \tag{16}$$

or

$$\psi_{F,ab}=\frac{-\int_0^1 v_d W_d B\psi_d(\eta_d,0)d\eta_d}{(R+1)V}$$

$$=\frac{-2W}{W_d(R+1)Gz_m}\sum_{m=0}^{\infty}\frac{e^{-\lambda_m}S_{d,m}}{\lambda_m}\{F'_{d,m}(1)-F'_{d,m}(0)\} \tag{17}$$

Moreover, the mixed dimensionless concentration at the end of the two outer subchannels are calculated by

$$\psi_{L,ab}=\frac{\frac{R}{R+1}\int_0^1 v_a W_a B\psi_a(\eta_a,0)d\eta_b-\int_0^1 v_a W_a B\psi_a(\eta_a,1)d\eta_b}{V}$$

$$=\frac{-2RW}{W_a(R+1)Gz_m}\sum_{m=0}^{\infty}\frac{e^{-\lambda_m}S_{a,m}}{\lambda_m}\{F'_{a,m}(1)-F'_{a,m}(0)\}$$

$$-\frac{2W}{W_aGz_m}\sum_{m=0}^{\infty}\frac{S_{a,m}}{\lambda_m}\{F'_{a,m}(1)-F'_{a,m}(0)\} \tag{18}$$

or

$$\psi_{L,cd}=\frac{\frac{R}{R+1}\int_0^1 v_d W_d B\psi_d(\eta_d,0)d\eta_d-\int_0^1 v_d W_d B\psi_d(\eta_d,1)d\eta_d}{V}$$

$$=\frac{-2RW}{W_d(R+1)Gz_m}\sum_{m=0}^{\infty}\frac{e^{-\lambda_m}S_{d,m}}{\lambda_m}\{F'_{d,m}(1)-F'_{d,m}(0)\}$$

$$-\frac{2W}{W_dGz_m}\sum_{m=0}^{\infty}\frac{S_{d,m}}{\lambda_m}\{F'_{d,m}(1)-F'_{d,m}(0)\} \tag{19}$$

3. Single- and double-pass devices

The single- and double-pass devices without external recycle are shown in Figs. 2 and 3, respectively. The dimensionless outlet concentrations for the double-pass devices (θ_F) and single-pass devices ($\theta_{0,F}$) were obtained in terms of mass-transfer Graetz number (Gz_m), eigenvalues (λ_m and $\lambda_{0,m}$), expansion coefficients ($S_{a,m}, S_{b,m}$ and $S_{0,m}$), channel thickness ratio (β) and eigenfunctions ($F_{a,m}(\eta_a)$, $F_{b,m}(\eta_b)$ and $F_{0,m}(\eta_0)$) by following the same mathematical treatment performed in the previous section. The results are

$$\theta_F=1-\psi_F=\frac{1}{Gz_m}\left[\sum_{m=0}^{\infty}\frac{(1-e^{-\lambda_m})W}{\lambda_m W_a}S_{a,m}F'_{a,m}(0)\right.$$

$$+\sum_{m=0}^{\infty}\frac{(1-e^{-\lambda_m})W}{\lambda_m W_b}S_{b,m}F'_{b,m}(0)\Bigg] \quad (20)$$

and

$$\theta_{0,F}=1-\psi_{0,F}=\frac{1}{Gz_m}\Bigg[\sum_{m=0}^{\infty}\frac{(1-e^{-\lambda_{0,m}})}{\lambda_{0,m}}S_{0,m}F'_{0,m}(0) + \sum_{m=0}^{\infty}-\frac{(1-e^{-\lambda_{0,m}})}{\lambda_{0,m}}S_{0,m}F'_{0,m}(1)\Bigg] \quad (21)$$

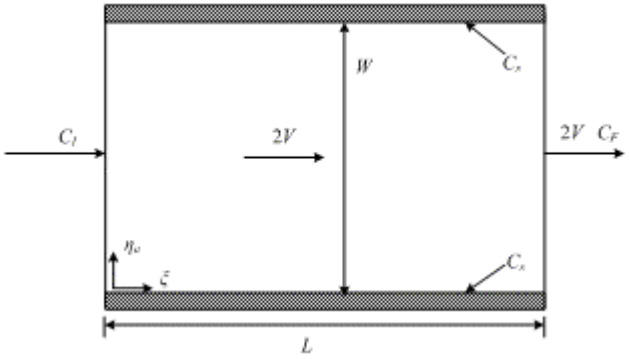

Fig.2 Single-pass devices

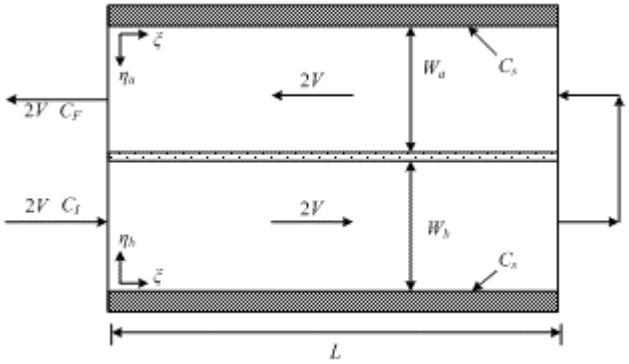

Fig.3 Double-pass devices

4. Mass transfer efficiency

The average Sherwood number is defined as

$$\overline{Sh}=\frac{\overline{k_m}W}{D} \quad (22)$$

where the average mass transfer coefficient is defined as

$$N=\overline{k_m}(2BL)(C_s-C_I) \quad (23)$$

By using the overall mass balance, the the average mass transfer coefficient can be determined by

$$\overline{k_m}(2BL)(C_s-C_I)=2V(C_F-C_I) \quad (24)$$

or

$$\overline{k_m}=\frac{2V}{2BL}\left(\frac{C_F-C_I}{C_s-C_I}\right)=\frac{2V}{2BL}(1-\psi_F) \quad (25)$$

Substituting Eq. (25) into Eq. (22) gives

$$\overline{Sh}=\frac{\overline{k_m}W}{D}=\frac{2VW}{2DBL}(1-\psi_F) = 0.5Gz_m(1-\psi_F)=0.5Gz\theta_F \quad (26)$$

Similarly, for a single-pass device

$$\overline{Sh}=\frac{\overline{k_{m,0}}W}{D}=\frac{2VW}{2DBL}(1-\psi_{0,F}) = 0.5Gz_m(1-\psi_{0,F})=0.5Gz\theta_{0,F} \quad (27)$$

The mass transfer efficiency improvement, I_m, by employing a multi-pass device is best illustrated by calculating the percentage increase in mass-transfer rate, based on that of a single-pass device with same working dimensions and without external recycle and any permeable barrier inserting

$$I_m=\frac{\overline{Sh}-\overline{Sh_0}}{\overline{Sh_0}}\times 100\%=\frac{\psi_{0,F}-\psi_F}{1-\psi_{0,F}}\times 100\% \quad (28)$$

5. Power consumption increment

The friction loss in the conduits can be estimated by

$$\ell w_f=\frac{2f\bar{v}^2L}{D_e} \quad (29)$$

where $\bar{v}$ and D_e refer the average velocities in the conduits and the equivalent diameters of the conduits, respectively. The friction factor f in the Eq. (29) is a function of Reynolds number, Re, as $f=24/\mathrm{Re}$ for the laminar flow and parallel-plate conduits. The equivalent diameters of the conduits for the single- and multi-pass device in the present studies are

$$D_{e,0}=2W \quad (30)$$

and

$$D_{e,a}=2W_a,\ D_{e,b}=2W_b,\ D_{e,c}=2W_c,\ D_{e,d}=2W_d \quad (31)$$

respectively. The power consumption increment, I_P, can be defined as

$$I_P=\{[(R+1)\ell w_{f,a}+\ell w_{f,b}+\ell w_{f,c}+(R+1)\ell w_{f,d}] -(2\ell w_{f,0})\}/2\ell w_{f,0} \quad (32)$$

Substitution of Eqs. (29)-(31) and the average velocity into Eq. (32) results in

$$I_P=\frac{(R+1)^2}{2}\left(\frac{W}{W_a}\right)^3+\frac{1}{2}\left(\frac{W}{W_b}\right)^3-1 \quad (33)$$

6. Results and discussions

The mass transfer equation in the multi-pass mass exchangers with external recycle and constant wall concentration has been developed and solved by using the orthogonal expansion technique and with the eigenfunctions expanding in terms of an extended power series. There two conflict effects are created by applying the recycle concept to the multi-pass devices. The desired effect is the increase of the convection mass

transfer coefficient while the undesired one is the decrease of the mass transfer driving force (concentration gradient). The mass transfer efficiency can be improved when the first effect compensate the last one.

The calculating results of the dimensionless outlet concentration are presented in Figs. 4 and 5. The dimensionless outlet concentration increases with decreasing the recycle ratio and subchannel thickness ratio as shown in Fig. 4. The large value of the parameter of permeable barrier, γ, represents that the solute can more easily transport through the permeable barrier. Therefore, Fig. 5 illustrates that the dimensionless outlet concentration increases with increasing the parameter of permeable barrier. Moreover, due to the short residence time for the large mass-transfer Graetz number, Gz_m, (high volumetric flow rate or short conduit length), the dimensionless outlet concentration decreases with increasing Gz_m as indicated in Figs. 4 and 5. The average Sherwood number versus mass- transfer Graetz number with the subchannel thickness ratio as a parameter for R = 5 is shown in Fig. 6. It is observed from Fig. 6, the average Sherwood number increases with increasing Gz_m but decreases with increasing subchannel thickness ratio. Figure 7 shows that the higher average Sherwood numbers were obtained in this work than those obtained in the previous work [8].

The mass transfer efficiency improvement, I_m, for the multi-pass mass exchanger with external recycle was calculated by Eq. (28) and the results are shown in Table 1. The mass transfer efficiency improvement, as observed from Table 1, increases with increasing Gz_m but decreases with increasing R and β. The operations of recycle concept and multi-pass design not only improve the mass transfer efficiency but also increase the power consumption. As shown in Eq. (33), the power consumption increment, I_p, does not depend on Graetz number but increases with recycle ratio and as β goes away from 1, especially for $\beta > 1$. The calculating results for I_p are presented in Table 2. By considering both the mass transfer efficiency and the power consumption increment, say I_m / I_p, there exits the optimal operating condition as shown in Fig. 8. The positive values of I_m / I_p mean that the mass transfer rate of multi-pass mass exchanger with external recycle are better than that of single-pass devices without external recycle.

7. Conclusion

The mathematical formulation of the new multi-pass mass exchangers with external recycle has been developed in present study. The analytical solutions were obtained by using the orthogonal expansion technique with the eigenfunction expanding in power series. The calculating results show that the multi-pass design and the external recycle operation can enhance the mass transfer rate of the mass exchangers. Comparing to the single-pass devices, the mass transfer rate of the multi-pass devices with external recycle increases with increasing mass-transfer Graetz number and the parameter of the permeable barriers but decreases with increasing recycle ratio and the subchannel thickness ratio. Moreover, comparing to the previous work [8], the improvement of device performance is obtained in this work. In the economic sense, there exits an optimal operating condition by considering I_m / I_p as indicated in Fig. 8.

Acknowledgement

The authors wish to thank the Chinese National Science Council for its financial support.

References

[1] R.K. Shah, & A.L. London, *Laminar flow forced convection in ducts* (Academic Press, New York, 1978).

[2] R.F. Barron, X. Wang, R.O. Warrington, & T. Ameel, Evaluation of the eigenvalues for the Graetz problem in slip-flow, *Int. Commun. Heat Mass Transf.*, *23*, 1996, 563-574.

[3] E. Papoutsakis, & D. Ramkrishna, Conjugated Graetz problems. I: General formalism and a class of solid-fluid problems, *Chem. Eng. Sci.*, *36*, 1981, 1381-1390.

[4] X. Yin, & H. H. Bau, The conjugated Graetz problem with axial conduction, *Trans. ASME*, *118*, 1996, 482-485.

[5] M. Sato, & M. Goto, Gas absorption in water with microchannel devices, *Sep. Sci. Tech. 39*, 2004, 3163-3167.

[6] A. Weiberg, H.H. Bau, & J.N. Zemel, Analysis of microchannels for integrated cooling, *Int. J. Heat Mass Transf.*, *35*, 1992, 2465-2474.

[7] C. D. Ho, H. M. Yeh, & Y. C. Tsai, Improvement in performance of multi-pass laminar counterflow heat exchangers with external refluxes, *Int. J. Heat Mass Transfer*, *45*, 2002, 3529-3547.

[8] C.D. Ho, & J.W. Tu, Multiple-pass flow mass transfer in a parallel-plate channel by inserting permeable barriers for improved device performance, *J. Chem. Eng. Japan*, *37*(1), 2004, 45-58.

[9] A.G. Jones, Liquid circulation in a drift-tube bubble column, *Chem. Eng. Sci.*, *40*, 1985, 449-462.

[10] C.D. Ho, H.M. Yeh & J.J. Guo, An analytical study on the enrichment of heavy water in the continuous thermal diffusion column with external refluxes, *Sep. Sci. Tech.*, *37*, 2002, 3129-3153.

Nomenclature

B conduit width, *m*

C concentration in the stream, mol/m^3
D ordinary diffusion coefficient, m^2/s
D_e equivalent diameter of the conduit, *m*
F_m eigenfunction associated with eigenvalue λ_m
f friction factor
Gz_m mass-transfer Graetz Number, $2VW/DBL$
I_m improvement of mass transfer, defined by Eq. (28)
I_p power consumption increment, defined by Eq. (32)
k_m average convection mass-transfer coefficient, m/s
L conduit length, *m*
ℓw_f friction loss in conduit, $N \cdot m/kg$
N mass transfer rate, $mole \cdot s$
P power consumption, $N \cdot m/s$
Re Reynolds number
S_m expansion coefficient associated with λ_m
$\overline{Sh}$ average Sherwood number
V input volume flow rate of fluid, m^3/s
v velocity distribution of fluid, *m/s*
$\bar{v}$ average velocity of fluid, *m/s*
W distance between two parallel plates, *m*
x transversal coordinate, *m*
z longitudinal coordinate, *m*

Greek letters

β ratio of channel thickness, $W_a/W_b = W_d/W_c$
γ the parameter of the permeable barrier, $\gamma = \varepsilon(W/\delta)$
δ thickness of the permeable barrier, *m*
ε permeability of the permeable barrier
η transversal coordinate, *x*/*W*
θ dimensionless concentration, $(C - C_I)/(C_S - C_I)$
λ_m eigenvalue
μ viscosity of the fluid, $kg/m \cdot s$
ξ longitudinal coordinate, *z*/*L*
ρ density of the fluid, kg/m^3
ψ dimensionless concentration, $(C - C_S)/(C_I - C_S)$

Subscripts

a the channel *a*
b the channel *b*
c the channel *c*
d the channel *d*
F at the outlet
I at the inlet
L at the end of the channel
0 in a single-pass device without recycle
s at the wall surface

Table 1. The mass transfer efficiency improvement with the channel thickness ratio as a parameter γ =10

	R = 1		
I_m	$\beta_{ab}=\beta_{cd}=1/3$	$\beta_{ab}=\beta_{cd}=1$	$\beta_{ab}=\beta_{cd}=3$
Gz_m=1	0.05	0.05	0.05
Gz_m=10	72.88	49.75	30.28
Gz_m=100	308.39	137.64	69.47
Gz_m=1000	393.20	157.71	76.76
	R = 5		
I_m	$\beta_{ab}=\beta_{cd}=1/3$	$\beta_{ab}=\beta_{cd}=1$	$\beta_{ab}=\beta_{cd}=3$
Gz_m=1	0.03	-0.33	-1.33
Gz_m=10	56.50	30.32	11.45
Gz_m=100	279.60	121.38	56.61
Gz_m=1000	380.75	147.58	67.18

Table 2. The power consumption increment with R and β as parameters

	I_p		
R	β =1/3	β =1	β =3
1	293	159	1033
3	2455	799	4180
5	6740	1951	9452

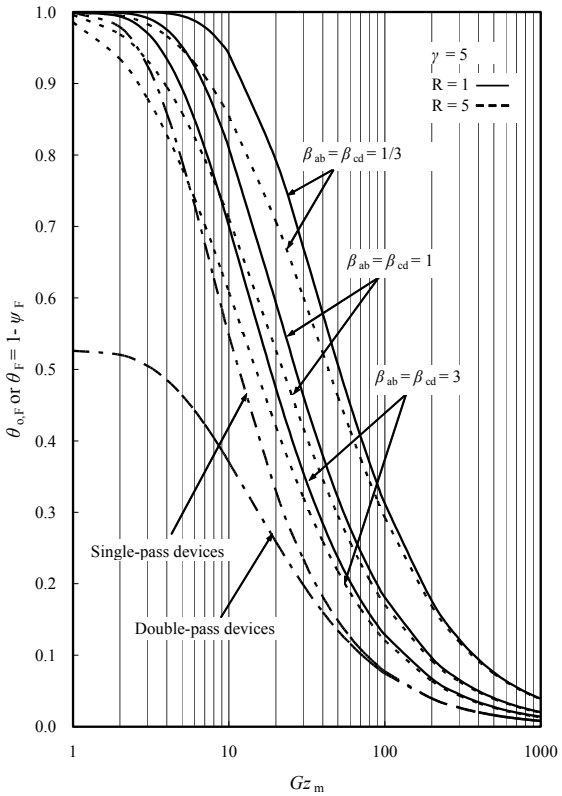

Fig. 4. Dimensionless outlet concentration vs. Gz_m with β_{ab} (or β_{cd}) as a parameter; R = 1 and 5.

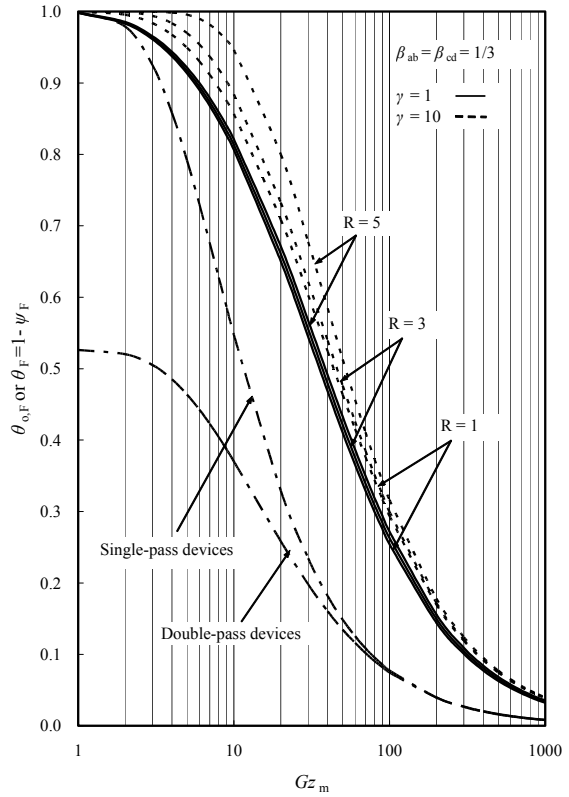

Fig. 5. Dimensionless outlet concentration vs. Gz_m with recycle ratio as a parameter; γ =1 and 10.

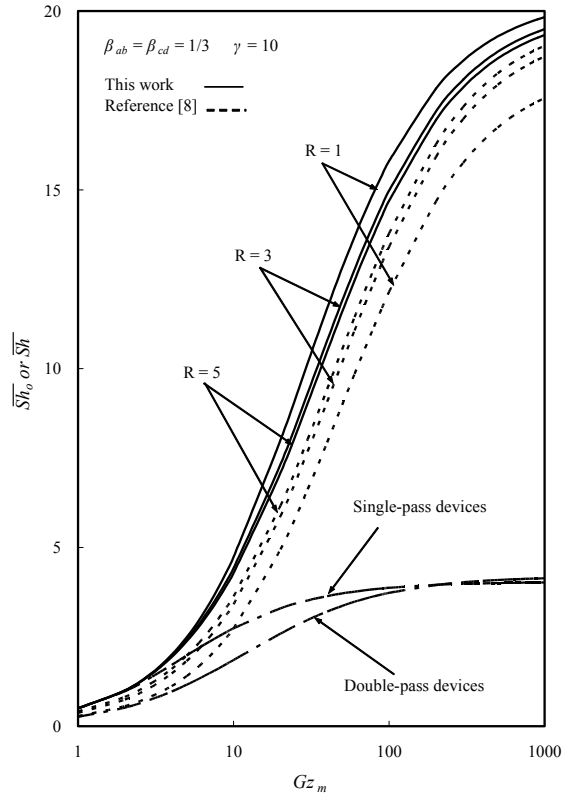

Fig. 7. The comparison of $\overline{Sh}$ obtained in this work and reference [8] with R as a parameter.

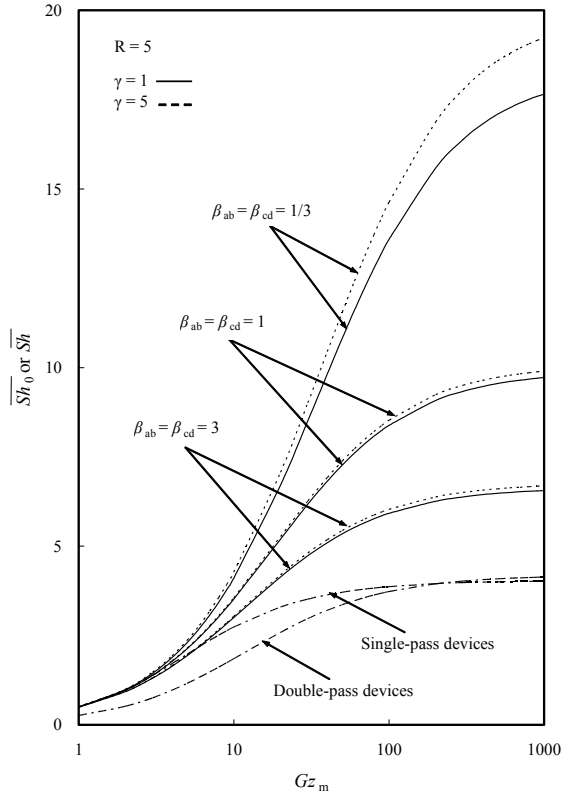

Fig. 6. Average Sherwood number vs. Gz_m with β_{ab} (or β_{cd}) as a parameter; γ =1 and 5.

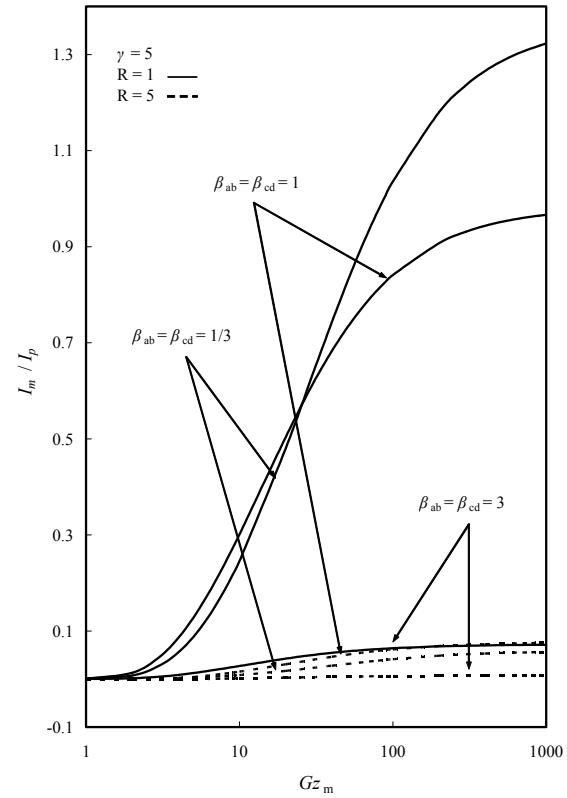

Fig. 8. The I_m / I_p vs. Gz_m with β_{ab} (or β_{cd}) as a parameter; R =1 and 5.